Nonspiral excitation waves beyond the eikonal approximation

Pavel K. Brazhnik and John J. Tyson
Department of Biology, Virginia Polytechnic Institute and State University, Blacksburg, Virginia 24061
(Received 15 May 1996)

Exact nonplanar traveling solutions for the kinematic model of autowaves in excitable media are constructed using a nonlinear velocity-curvature relation that is more realistic than the linear (eikonal) approximation. The physically unrealistic self-crossing fronts, found earlier in the eikonal approximation, are replaced by noncrossing fronts with cusplike singularities that are reminiscent of ''cellular'' flame structures. The new solutions put restrictions on possible autowave refraction and reflection regimes found in the eikonal approximation. A possible role of the unstable branch of the velocity-curvature relation in removing the cusplike singularities from the present solutions is discussed. [S1063-651X(96)04710-1]

PACS number(s): 03.40.Kf

I. INTRODUCTION

From the realm of nonlinear dissipative systems that spontaneously generate spatially and temporally ordered structures, we are studying waves propagating in so-called excitable media (EM)—the model prototype of many actual biological and chemical media [1–3]. The mathematical theory of EM is based on systems of nonlinear partial differential equations (PDE's) of reaction-diffusion type [2,4]. Two component models

$$\frac{\partial u}{\partial t} = D_u \Delta u + f(u,v), \qquad \frac{\partial v}{\partial t} = D_v \Delta v + g(u,v) \tag{1}$$

are usually satisfactory to reproduce the basic features of EM. The dependent variables u and v are called the excitation and recovery variables, respectively. $D_{u,v}$ are their corresponding diffusion coefficients, Δ is the Laplacian operator in two or three spatial dimensions (2D or 3D), and f and g are appropriate nonlinear kinetic functions. Under appropriate conditions, these equations admit solutions describing propagating waves of excitation (autowaves) with interesting geometrical properties.

In the extensive literature of EM two kinds of steady-state structures (structures propagating at constant speed with invariant shape) dominate: moving plane fronts and rotating spiral waves. In our recent theoretical work we have shown, using a kinematic approach [5], that in 2D EM several other steady-state propagating solutions exist. One example is V-shaped waves, which have been subsequently studied experimentally in the Belousov-Zhabotinsky (BZ) reaction and in numerical experiments with PDE's [6]. Three other solutions found produce self-crossing fronts (containing one or an infinite number of loops) and, therefore, could not be identified with any stationary autowave pattern in homogeneous EM. But they turned out to be crucially important for constructing steady-state patterns in piecewise inhomogeneous EM [5,7,8]. The looplike structure of these solutions is, in fact, an artifact generated by extrapolating the linear approximation for the velocity-curvature relation of propagating fronts beyond the region of its applicability.

In this paper we improve the kinematic theory of steady-state autowaves by replacing the eikonal approximation with a more realistic nonlinear dependence of local front velocity on front curvature. The nonlinear relation includes a critical curvature, beyond which sustained wave propagation is impossible, and an unstable branch of slow-speed waves. We construct all nonspiral steady-state wave-front configurations, study their properties and discuss the physical interpretation of these solutions. The consequences of critical curvature for autowave refraction-reflection are investigated.

II. MODEL AND ITS SOLUTIONS IN THE EIKONAL APPROXIMATION

The strong nonlinearity of PDE models of EM does not allow for their exact solution and complicates approximate analytical analysis in the most interesting 2D and 3D cases. To get results, numerical integration of system (1) has become very popular. Alternatively, large-scale dynamics of solitary (noninteracting) fronts in 2D and 3D are often successfully treated by geometrical models [4,9–13], the most elaborate of which is the so-called ''kinematic approach.'' The results of kinematic theory are often in good agreement with numerical [14,15] and approximate analytical [16] calculations on PDE models, and it has proved itself to have predictive power [6,17,18]. The foundations of kinematic theory can be found in [3,4,9,19]. Below we outline briefly only those elements of the approach that are necessary for understanding this paper.

A. Model equations

The kinematic model is based on the assumption that shape changes of a solitary, modestly curved front can be satisfactorily described without keeping track of the dynamics of the excitation pulse. Therefore the kinematic description reduces a pulse structure in 1D to a single point, so that an excited region in a 2D EM is conceived as an infinitely thin curved line with a normal vector pointing in the direction of propagation. Analysis of PDE systems shows that diffusion terms make the local velocity of the front V depen-

 © 1996 The American Physical Society

dent on front curvature k, $V=V(k)$. It is convenient then to specify the shape of the wave front line by an intrinsic equation $k=k(l)$ that relates the curvature of the front to arc length along the front l. Generally speaking, a propagating front changes its shape with time t and therefore $k=k(l,t)$. We consider only steady-state fronts (those that propagate with invariable shapes) for which $\partial k/\partial t=0$. Then $k(l)$, for infinitely extended endless fronts [20], satisfies the following integro-differential equation,

$$k(l)\int_0^l k(\xi)V(k(\xi))d\xi+\frac{dV(k(l))}{dl}=\omega. \tag{2}$$

By putting further the right-hand side equal to zero ($\omega=0$), we exclude from present consideration spiral-like solutions for which $\omega=\text{const}>0$ [9]. Notice also that such a choice places the origin ($l=0$) at a point on the front where its velocity is extremal, $(dV/dl)_{l=0}=0$. A boundary condition $k(0)$, consistent with the extremal-velocity condition, has to be specified in order to determine a unique solution of Eq. (2).

The intrinsic equation $k(l)$ defines the front curve uniquely except for its position and orientation on a plane. Parametric representation of an actual front line in the Cartesian frame of reference can be constructed from the intrinsic equation by a standard procedure:

$$x(l)=\int_0^l \sin(\theta(\xi))d\xi,$$

$$y(l)=\int_0^l \cos(\theta(\xi))d\xi, \tag{3}$$

where x and y are Cartesian coordinates of the front line, and

$$\theta(l)=-\int_0^l k(\xi)d\xi \tag{4}$$

is the angle between the tangent to the wave front at the point l and the axis OY, taken as positive if measured clockwise from the positive direction of the axis OY.

For noncirculating solutions a simplification of the integro-differential equation (2) turns out to be possible. Multiplying Eq. (2) by $V(k)$, integrating once, and changing variables from l to θ, we get

$$\left[\int_0^{\theta(l)} V(\theta)d\theta\right]^2+[V(\theta)]^2=[V(0)]^2, \tag{5}$$

where $V(0)$ denotes the normal velocity of the wave at $\theta=l=0$ and is to be distinguished from V_0, the velocity at $k=0$. The solution of Eq. (5) satisfying the condition $(dV/dl)_{l=0}=0$ is

$$V(\theta)=V(0)\cos(\theta). \tag{6}$$

Equation (6) implies that a steady-state wave must move as a whole along the X axis with a speed $V(0)$. Differentiating Eq. (6) with respect to l, gives

$$\frac{dV}{dl}=k(l)\sqrt{[V(0)]^2-V^2}, \tag{7}$$

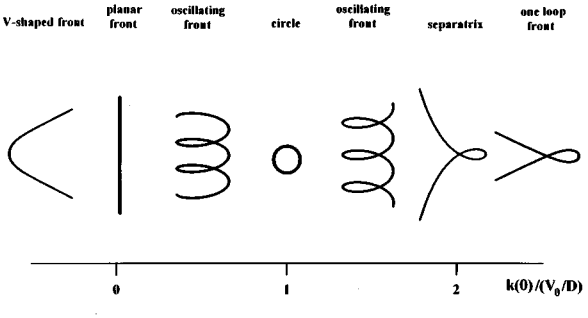

FIG. 1. Shapes of steady-state autowave fronts corresponding to solutions of the kinematic model in the eikonal approximation. Solutions are parametrized by the ''initial'' value $k(0)$. Properties of each pattern are discussed in the text.

where V depends on l through k: $V=V(k(l))$. For a given $V=V(k)$, Eq. (7) can be rewritten as a first-order differential equation for $k(l)$.

B. Solutions of the kinematic model in eikonal approximation

It follows from both experiments [21] and theoretical considerations [22–25] that the dependence of local front velocity V on curvature k, for modestly curved fronts, can be taken as linear

$$V(k)=V_0-Dk. \tag{8}$$

Here V_0 is the velocity of the planar front ($k=0$), and D is the diffusion coefficient of the excitation variable. Substituting Eq. (8) into Eq. (7) gives

$$D\frac{dk}{dl}=\mp k(l)\sqrt{[V_0-Dk(0)]^2-[V_0-Dk]^2}. \tag{9}$$

Solutions of this equation parametrized by the ''initial'' value $k(0)$ have been studied in [5].

For $k(0)<0$, the front propagates in the form of a V-shaped wave [15,17]. Its profile is given by the soliton-type expression

$$k(l)=-\frac{1}{D}\frac{[V(0)]^2-V_0^2}{V_0+V(0)\cosh\left(\dfrac{l}{l_0}\right)},\quad -\infty<l<\infty, \tag{10}$$

with characteristic length $l_0=D\{|[V(0)]^2-V_0^2|\}^{-1/2}$. The curvature of this front is always negative and its magnitude decreases exponentially to zero as $|l|$ goes to infinity. The asymptotic angle between the wings follows directly from Eq. (6),

$$\alpha=\pi-2\,\theta(l\to\pm\infty)=2\arcsin\left[\frac{V_0}{V(0)}\right]. \tag{11}$$

The V-shaped wave moves uniformly, with velocity $V(0)>V_0$ (i.e., faster than a planar front), from left to right as shown in Fig. 1. As $k(0)\to 0$, the angle between asymptotes of the V-shaped wave increases to π and the velocity of the pattern decreases to V_0, that is the pattern converts into a plane wave ($k=0$).

Positive $k(0)$ produces space-oscillating fronts described by

$$k(l) = -\frac{1}{D}\frac{[V(0)]^2 - V_0^2}{V_0 + V(0)\cos\left(\frac{l}{l_0}\right)}. \tag{12}$$

As $k(0)$ increases from zero up to $k(0) \simeq V_0/D$, both the amplitude and period of the oscillations in front curvature decrease: the amplitude from V_0/D to zero, and period from infinity to $2\pi D/V_0$. The front propagates with a speed $V(0) < V_0$, from left to right as depicted in Fig. 1. At $k(0) = V_0/D$ the front degenerates to a standing ring of radius $1/k = V_0/D$. When $k(0)$ becomes greater than V_0/D and moves toward $2V_0/D$, the space-oscillating front appears again but now the behavior of its amplitude and period is opposite to that which took place when $k(0)$ ran from zero to V_0/D. Also the direction of front propagation reverses: the front moves from right to left in Fig. 1 with speed $|V(0)| < V_0$.

The value $k(0) = 2V_0/D$ corresponds to a separatrix solution, with algebraic soliton-type shape

$$k(l) = \frac{2V_0/D}{1 + \left(\frac{l}{D/V_0}\right)^2}. \tag{13}$$

This front retains only one loop and has asymptotically flat wings, $k(l \to \pm\infty) \to 0$, separated by an angle of π. The front moves with a speed V_0, from right to left in Fig. 1.

Increasing $k(0)$ beyond $2V_0/D$ retains the one-loop structure of the front but changes the asymptotic angle α between the wings $\alpha = 2\arcsin[V_0/|V(0)|]$, which goes to zero as $k(0) \to \infty$. The front still moves from right to left (Fig. 1), now with the velocity $|V(0)| > V_0$.

Linear stability analysis shows [5] that the solutions are stable with respect to small localized perturbations that disappear diffusively (with characteristic time D/V_0^2), traveling along the front towards regions of maximum curvature. Nonlocalized perturbation may lead to the formation of a pattern with new parameters.

III. SOLUTIONS BEYOND THE EIKONAL APPROXIMATION

The steady-state equation for curvature-driven fronts Eq. (7) is general in the sense that its derivation did not require us to specify the dependence $V(k)$. Thus, it allows for analytical study of wave kinematics beyond the eikonal approximation for systems where an analytical expression for $V(k)$ can be derived from corresponding PDE models or experiments.

A. The dependence of velocity on curvature

Experiments with chemical EM show [15,21] that the dependence $V(k)$ is linear only in a small region of positive curvature and in a larger region of negative curvature. More careful analytical [23] and numerical studies [22,24,25] of PDE's and cellular automaton models indicate that this velocity-curvature relation is nonlinear and exhibits a positive critical curvature k_{cr} beyond which propagation of a continuous front is impossible: the front breaks apart in those regions where its curvature exceeds the critical value [26].

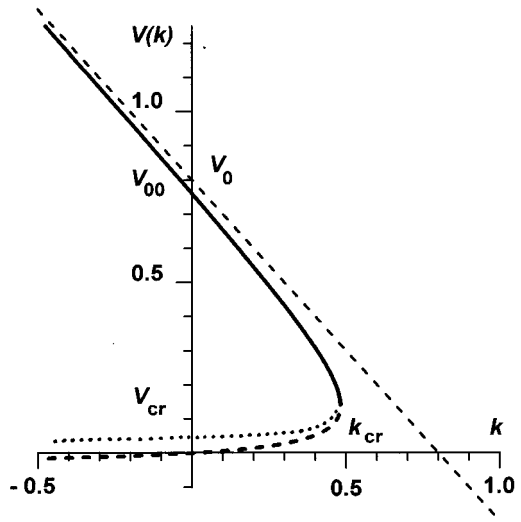

FIG. 2. The Zykov dependence of normal propagation velocity V on curvature k [Eq. (15)] is depicted by a thick line: stable branch by a solid line and unstable branch by a dashed line. The eikonal approximation is shown by a straight dashed line. The dotted line shows more realistic behavior of the unstable branch than predicted by Eq. (15). In this figure and later figures, all quantities have been scaled to dimensionless values. In particular, $D = 1$ and $V_0 = 0.8$.

An analytical evaluation of the nonlinear dependence of speed on curvature was given by Zykov for two-component reaction-diffusion systems containing a ''fast'' variable u and a ''slow'' variable v

$$\frac{\partial u}{\partial t} = D\Delta u + f(u,v), \qquad \frac{\partial v}{\partial t} = \epsilon g(u,v). \tag{14}$$

In this case the recovery variable v does not spread in space, e.g., a BZ medium with the catalyst immobilized in a gel [27], or neuromuscular tissue where v represents the local permeability of a membrane to transmembrane ionic currents [28].

Considering ϵ as a small dimensionless parameter, Zykov derived the following approximate relationship for speed V vs curvature k of traveling wave [13,23]:

$$V(k) = \frac{V_{00} - Dk}{2} \pm \left[\left(\frac{V_{00} - Dk}{2}\right)^2 - (\epsilon V_1)Dk\right]^{1/2}. \tag{15}$$

Here $V_{00} = V_0 - \epsilon V_1$, where V_0 is the velocity of a plane front in a medium with $\epsilon \to 0$ (the system with highest excitability), and V_1 is a first-order correction of the velocity for $\epsilon \neq 0$ (which must satisfy $V_1 \leqslant V_0/\epsilon$). The $+$ sign goes with the stable branch, depicted in Fig. 2 by a thick solid line, and the $-$ sign goes with the unstable branch depicted by a thick dashed line [29]. For negligibly small ϵ, the stable branch of Eq. (15) approaches the eikonal approximation. For nonzero

ϵ, Eq. (15) predicts a nearly linear dependence for negative curvatures and for positive curvatures close to zero. For more positive curvatures the relation $V(k)$ departs from linearity and finally, at the point where $dV/dk \to \infty$, exhibits the critical value for curvature k_{cr}, related to the parameter ϵ by the expression

$$k_{cr} = \frac{V_0}{D}\left[1 - \left(\frac{\epsilon V_1}{V_0}\right)^{1/2}\right]^2. \tag{16}$$

Thus, the critical curvature decreases with increasing contribution of v to the excitation process. No wave can propagate with curvature larger than critical. The portion of the front where curvature reaches the critical value propagates with nonzero velocity $V_{cr} = (V_{00} - Dk_{cr})/2$.

B. Phase plane analysis

Substituting Eq. (15) into Eq. (7) leads to the differential equation

$$\frac{dk}{dl} = \mp k\left(\frac{dk}{dV}\right)\sqrt{[V(0)]^2 - [V(k)]^2}, \tag{17}$$

where

$$\frac{dk}{dV} = -\frac{1}{D}\left\{1 - \frac{\epsilon V_1 (V_{00} + \epsilon V_1)}{[V(k) + \epsilon V_1]^2}\right\}$$

and at $\epsilon = 0$ the equation converts into Eq. (9). Before constructing exact solutions to Eq. (17), it is instructive to plot dk/dl vs k, in order to get an idea about the number and character of solutions we have to expect and specific features of the solutions with Zykov's velocity-curvature relation compared to the eikonal approximation solutions.

For the eikonal approximation ($\epsilon = 0$, and $dk/dV = -1/D$), a set of orbits is depicted in Fig. 3 by dashed lines. These orbits are parametrized by the ''initial'' condition $k(0)$. Arrows on orbits show the direction of increasing $|l|$. All orbits start at $(k(0), dk/dl = 0)$ because the initial value for dk/dl has been uniquely specified for all orbits as $(dk/dl)_{l=0} = 0$ by choosing $\omega = 0$ in Eq. (2). The phase space turns out to be partitioned into regions corresponding to qualitatively different ''motions'' depending on the value of the ''initial'' condition $k(0)$. Loops adjoined to the origin correspond to solution (10) and describe, for $k(0) < 0$, V-shaped waves, and for $k(0) > 2V_0/D$, one-loop fronts. Periodic orbits on the $k > 0$ half plane correspond to solution (12). The trivial steady state at the origin $k(0) = k(l) = 0$ corresponds to a plane wave, and the center at $(V_0/D, 0)$ gives a standing ring. Orbits exist for any initial value of $k(0)$ and cover the whole phase space except for the vertical axis.

When $\epsilon \neq 0$ orbits occupy only the half plane $(k < k_{cr}, dk/dl)$ [29]. These are depicted by solid lines in Fig. 3. In spite of the fact that Zykov's dependence $V(k)$ gives a curve which ends when $k = k_{cr}$, all orbits are continuous and smooth, and therefore the corresponding front intrinsic equations are expected to be continuous and smooth. Since the eikonal approximation and Zykov's dependence are almost identical for negative curvatures, orbits in the half plane $k < 0$ differ only slightly from each other and similarly for the region of positive k close to zero. Substantial rearrangement of orbits is limited to the half plane where curvature is much greater than zero. As Fig. 3 makes clear, the introduction of positive critical curvature does not destroy looplike and periodic orbits for $k > 0$ but flattens them at large curvatures so that the highest curvature they reach is k_{cr}, where dk/dl turns out to be zero. The latter fact indicates, in particular, that the branches with positive and negative l match each other smoothly at the point where $k = k_{cr}$. The standing ring predicted by the eikonal approximation disappears. In this case we have three different kinds of propagating solutions.

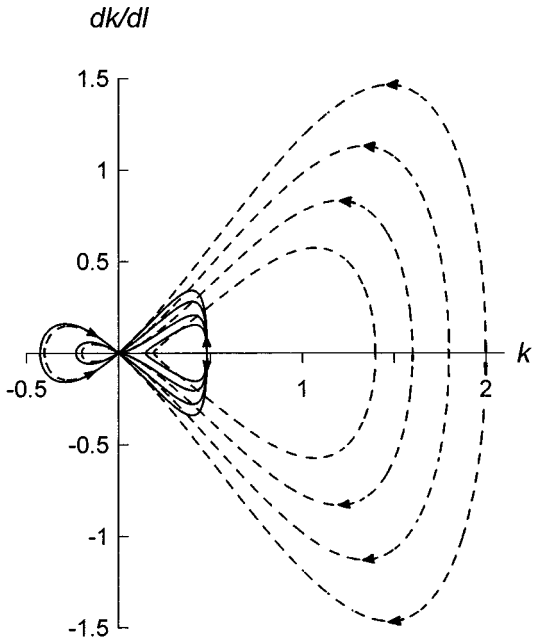

FIG. 3. Phase portrait of Eq. (7) for eikonal approximation Eq. (8) (dashed lines) and for Zykov's dependence (15) (solid lines). Parameter values are $D = 1$, $V_0 = 0.8$, $\epsilon V_1 = 0.04$. Arrows on curves indicate the flow of the trajectories when l runs from 0 to $\pm\infty$. Loops in the half plane $k < 0$ represent V-shaped waves for two different values of the initial condition: for eikonal curves $k(0) = -0.4$ and -0.2. Large loops in the half plane $k > 0$ correspond to two one-loop solutions $[k(0) = 2.0$ and $1.8]$, the separatrix solution $[k(0) = 1.6]$, and an oscillating solution $[k(0) = 0.2]$. The corresponding orbits for Zykov's dependence are shown as the solid lines.

C. Three types of solutions

In order to construct steady-state solutions for the kinematic model with Zykov's function $V(k)$ it is convenient to solve the front equation (7) expressing k as a function of V from Eq. (15)

$$k(V) = \frac{V(V_{00} - V)}{D(V + \epsilon V_1)}. \tag{18}$$

The front equation becomes

$$D\left[\frac{\frac{\epsilon V_1}{V_{00}}}{V\sqrt{[V(0)]^2 - V^2}} + \frac{\left(1 + \frac{\epsilon V_1}{V_{00}}\right)}{(V_{00} - V)\sqrt{[V(0)]^2 - V^2}}\right]\frac{dV}{dl} = 1. \tag{19}$$

The first term in the brackets does not depend on the value of ''initial'' condition $V(0)$ and after being integrated gives the contribution

$$-\frac{D}{V(0)}\left(\frac{\epsilon V_1}{V_{00}}\right)F(V),$$

$$\text{where } F(V)=\ln\left[\frac{V(0)}{V}+\left\{\left(\frac{V(0)}{V}\right)^2-1\right\}^{1/2}\right]. \quad (20)$$

The second term on the left-hand side is responsible for splitting solutions of Eq. (19) into three different categories depending on the ratio between V_{00} and $V(0)$.

(1) When $V(0)>V_{00}$, the second term in Eq. (19) can be integrated to

$$\frac{D\left(1+\frac{\epsilon V_1}{V_{00}}\right)F_1(V)}{\sqrt{[V(0)]^2-V_{00}^2}},$$

where

$$F_1(V)=\ln\left[\frac{V^2(0)-V_{00}V+\sqrt{\{[V(0)]^2-V_{00}^2\}\{[V(0)]^2-V^2\}}}{0.5V_{00}(V_{00}-V)}\right]. \quad (21)$$

The general solution for Eq. (19) then is

$$D\left[-\frac{\frac{\epsilon V_1}{V_{00}}}{V(0)}F(V)+\frac{1+\frac{\epsilon V_1}{V_{00}}}{\sqrt{[V(0)]^2-V_{00}^2}}F_1(V)\right]=l+L, \quad (22)$$

where constant L must be determined from initial conditions. Taking into account that $V(l=0)=V(0)$, we get a one-parameter family of solutions in the following form:

$$-\left(\frac{\epsilon V_1}{V_{00}}\right)\left(1-\left[\frac{V_{00}}{V(0)}\right]^2\right)^{1/2}F(V)+\left(1+\frac{\epsilon V_1}{V_{00}}\right)\ln\left[\frac{V^2(0)-V_{00}V+\sqrt{\{[V(0)]^2-V_{00}^2\}\{[V(0)]^2-V^2\}}}{V(0)(V-V_{00})}\right]=\frac{l}{l_0}. \quad (23)$$

Substituting Eq. (15) into the left-hand side of Eq. (23) provides now an intrinsic equation for the wave front line for given ''initial'' condition $k(0)<0$. This solution corresponds in Fig. 3 to the looplike orbit on the half plane $k<0$ and is depicted in Fig. 4 in the lower half plane together with the corresponding V-wave solution in the eikonal approximation. The slight difference of these solutions around the origin results in a slightly smaller asymptotic angle of the resulting V pattern ($\alpha=2\arcsin[V_{00}/V(0)]$) compared to the eikonal approximation [Eq. (11)].

In the phase plane the solution (22) for each $V(0)$ has two branches. The branch we have just studied starts at $l=0$ with normal velocity $V=V(0)$ and curvature $k(0)<0$, and ends with $V=V_{00}$ and $k=0$ when $l\to\infty$. Another branch starts at the origin and loops into the positive half plane $k>0$. The normal velocity of the front on this branch decreases from V_{00} at $k=0$ to V_{cr} at $k=k_{cr}$. Therefore, there is no point on the front that we can assign as $l=0$, with $V(l=0)=V(0)$, because $V(0)>V_{00}$ by assumption. We must parametrize the positively curved branch in a different way. Let s be the wave-front arc length measured from the point where the curvature reaches its critical value, $k(s=0)=k_{cr}$. Then the solution (23) becomes

$$-\left(\frac{\epsilon V_1}{V_{00}}\right)\left(1-\left[\frac{V_{00}}{V(0)}\right]^2\right)^{1/2}[F(V)-F(V_{cr})]+\left(1+\frac{\epsilon V_1}{V_{00}}\right)$$

$$\times[F_1(V)-F_1(V_{cr})]=\frac{s}{l_0}. \quad (24)$$

Several curves generated by Eq. (24) are depicted in Fig. 4 together with corresponding one-loop solutions of the eikonal approximation. Unlike solutions (23), solutions (24) differ from each other not by the value of its velocities (curvature) at $s=0$ but by its width at $s=0$, i.e., by $(d^2k/ds^2)_{s=0}$. This derivative is uniquely defined by $V(0)$ through the expression

$$\left(\frac{d^2k}{ds^2}\right)_{k=k_{cr}}=-\frac{2}{D}\frac{k_{cr}^2}{V_{cr}+V_1\epsilon}\{[V(0)]^2-V_{cr}^2\}. \quad (25)$$

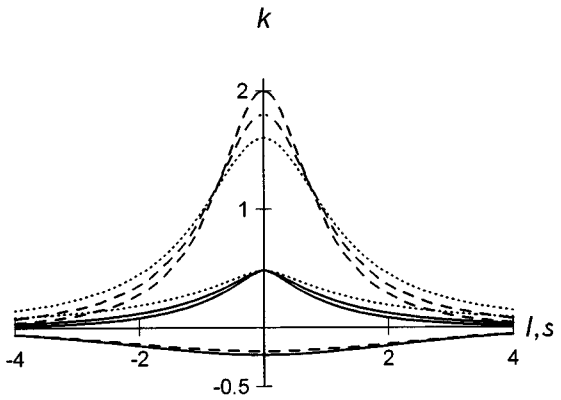

FIG. 4. Intrinsic equation curves $k=k(l)$ for the eikonal approximation (dashed lines) and for Zykov's velocity-curvature dependence (solid lines). Dotted curves are corresponding separatrix solutions. The upper group of curves in the upper half plane is evaluated in the eikonal approximation for initial conditions: $V(0)=-1.2$, $V(0)=-1$, and $V(0)=-0.8$ (from the top to the bottom). The lower group of curves in this half plane is the corresponding group of solutions for Zykov's dependence. Curves in the lower half plane are V-shaped waves for $V(0)=1$. Other parameters as in Fig. 3.

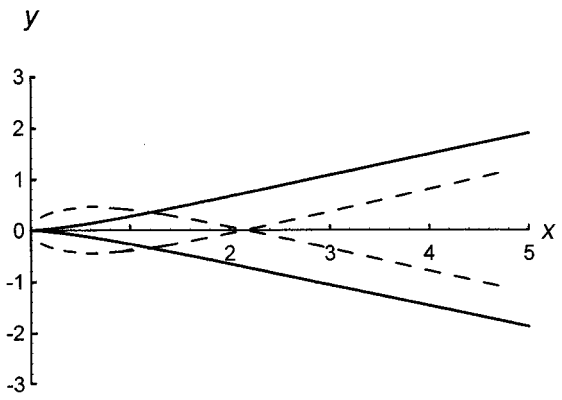

FIG. 5. The front line corresponding to solution (24) is depicted in the Cartesian frame of reference (solid line) together with the one-loop solution (10) for the eikonal approximation (dashed line). $V(0)=2$ and other parameters as in Fig. 3.

As $V(0)$ runs from V_{00} to infinity, the width of the curve $k(s)$ given intrinsically by Eq. (24) runs from its finite maximum value to zero. The front corresponding to this solution is depicted in the Cartesian frame of reference in Fig. 5, together with the one-loop front of the eikonal approximation. Taking into account the existence of a critical curvature above which sustained wave propagation is impossible, we find that the loops attributable to breakdown of the eikonal approximation are converted into singular cusps. Since the entire pattern propagates along the X axis at a velocity $V(0)$, it must be true that

$$\frac{V(s\rightarrow\infty)}{\sin(\alpha/2)}=\frac{V(s\rightarrow 0)}{\sin(\alpha_{\mathrm{cusp}}/2)}=V(0),$$

where α is the angle subtended by the wings of the pattern and α_{cusp} is the cusp angle. Therefore, $\alpha=2\arcsin[V_{00}/V(0)]$ can be related to the width of the solution through Eq. (25) and $\alpha_{\mathrm{cusp}}=2\arcsin[V_{\mathrm{cr}}/V(0)]$ is determined by the critical curvature.

(2) For $V(0)=V_{00}$, there exists, besides the trivial solution $k(l)=0$ corresponding to a plane front, also a nontrivial separatrix solution. For the separatrix solution it is again convenient to measure arc length s from the point where $k(s=0)=k_{\mathrm{cr}}$. Then the solution of Eq. (19) becomes

$$-\left(\frac{\epsilon V_1}{V_{00}}\right)[F(V)-F(V_{\mathrm{cr}})]+\left(1+\frac{\epsilon V_1}{V_{00}}\right)\left[\left(\frac{V_{00}+V}{V_{00}-V}\right)^{1/2}-\left(\frac{V_{00}+V_{\mathrm{cr}}}{V_{00}-V_{\mathrm{cr}}}\right)^{1/2}\right]=\frac{s}{D/V_{00}}. \tag{26}$$

Using Zykov's $V(k)$, we obtain the separatrix (lower dotted) curve depicted in Fig. 4. The front line described by this solution is shown in Fig. 6 together with its counterpart in the eikonal approximation. Again, the looped front is replaced by one with a singular cusp. The cusp angle for this limiting case is given by $\alpha_{\mathrm{cusp}}=2\arcsin[V_{\mathrm{cr}}/V_{00}]$. The pattern propagates with the velocity of a planar front.

(3) For the case $V_{\mathrm{cr}}<V(0)<V_{00}$, Eq. (19) gives the family of oscillating solutions

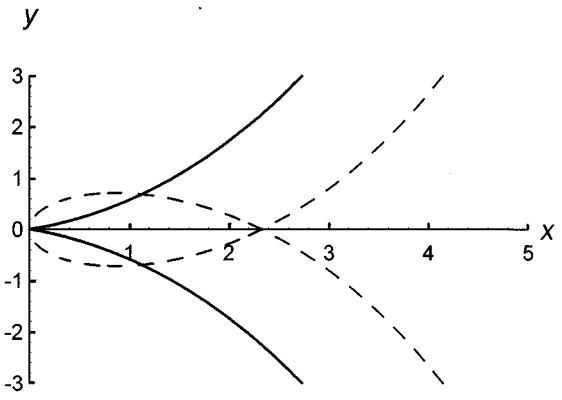

FIG. 6. The front-line corresponding to solution (26) is depicted in the Cartesian frame of reference (solid line) together with the separatrix solution (13) for the eikonal approximation (dashed line). In both case, $(dy/dx)\rightarrow\infty$ as $l\rightarrow\pm\infty$.

$$-\frac{D}{V(0)}\left(\frac{\epsilon V_1}{V_{00}}\right)F(V)+\frac{D\left(1+\dfrac{\epsilon V_1}{V_{00}}\right)}{\sqrt{V_{00}^2-[V(0)]^2}}\arccos\times\left[-\frac{[V(0)]^2-V_{00}V}{V(0)(V_{00}-V)}\right]=l. \tag{27}$$

Here we have placed the point $l=0$ where the curvature of the front is minimal. Equations (27) and (15) generate $k(l)$ depicted in Fig. 7, along with the corresponding eikonal approximation. The front lines implied by these equations are shown in Fig. 8. Again, looped fronts of the eikonal approximation are converted into singular cusps by Zykov's dependence. The amplitude and period of the front-line space oscillations can be determined from Eqs. (3), (6), and (18) and depend, apart from V_0 $V(0)$, and D, also on the value of the critical curvature. For example, the amplitude A, the distance from the cusp to the top of the hump, is given by

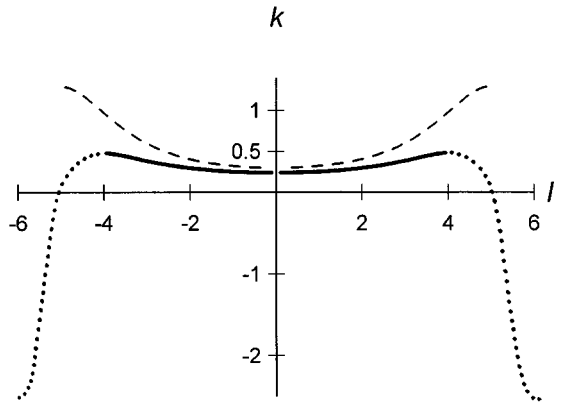

FIG. 7. One period of the intrinsic equation for solution (27) (solid line) together with its counterpart in the eikonal approximation (dashed line). The initial condition is chosen as $V(0)=0.5$. Other parameters as in Fig. 3. Dotted lines are portions of the intrinsic equation produced by the unstable brunch of $V(k)$ (dotted line in Fig. 2).

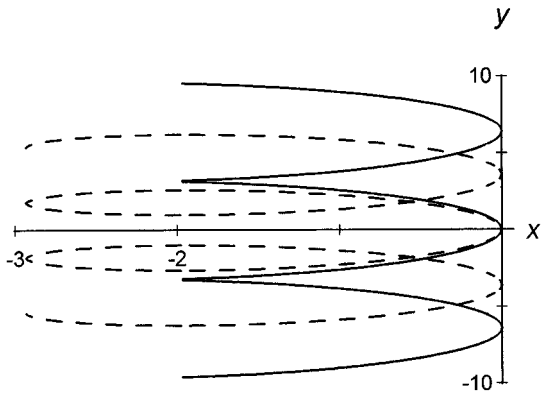

FIG. 8. Three periods of the front line corresponding to solution (27) are depicted in the Cartesian frame of reference (solid line) together with the oscillating solution (12) for the eikonal approximation (dashed line).

$$A=\frac{D}{V(0)}\left|\log\left[\frac{V_{00}-V_{\rm cr}}{V_{00}-V(0)}\right]-\frac{\epsilon}{V_{00}}\log\left[\frac{V_{00}-V_{\rm cr}}{V_{00}-V(0)}\left(\frac{V(0)}{V_{\rm cr}}\right)\right]\right|. \tag{28}$$

Both the amplitude and the period of the front-line oscillations decrease from infinity to zero when $V(0)$ runs from V_{00} to $V_{\rm cr}$. The cusp angle is given by the same expression as for the solution (24). The theory of stability developed in [5] implies that the solutions we have found are geometrically stable.

IV. DISCUSSION

The solutions we have found describe possible steady-state wave-front configurations in 2D unrestricted EM. It turns out that some of them are also relevant to possible regimes in EM bounded by straight impenetrable boundaries. No flux at an impenetrable boundary implies that a steady-state propagating front must always meet the boundary orthogonally. For EM restricted to a half plane only three regimes from those we have constructed can satisfy the required boundary conditions: (1) a plane wave propagating in the direction parallel to the boundary; (2) a ''tilted'' plane wave constituting half of a V-shaped wave whose line of symmetry coincides with the boundary; (3) an oscillating front propagating parallel to the boundary and touching the boundary at the top of its hump. For an EM confined inside an infinitely long band (two parallel impenetrable boundaries), according to our theory, two steady-state regimes are possible: a plane wave oriented perpendicular to the boundaries, and an oscillating front propagating along the band and touching the boundaries at the tops of its humps.

In [5,7,8] we have shown that solutions in unrestricted EM are vital ingredients of autowave patterns in layered media. In particular, in [8] we showed that, when an autowave travels through a semipenetrable boundary into a less excitable medium, it is refracted at an angle that depends on the discontinuity in excitability. According to the eikonal approximation, the angle of refraction can run from zero to $\pi/2$ meaning that refraction is observable for negligibly small differences and for arbitrarily large differences in excitability. Formally this conclusion follows from the fact that solution (10), used as a piece of a steady-state incident wave, can be smoothly concatenated with a plane-wave fragment of a steady-state refracted wave at any angle within the interval $(\theta_{\rm incident},\ \pi/2-\theta_{\rm incident})$. Accounting for critical curvature replaces solution (10) by Eq. (23). The front-line corresponding to Eq. (23) permits only a restricted variation of the angle between the tangent to the front and the axis OX (see Fig. 5), namely, it runs from $\theta(k=0)$ up to $\theta(k=k_{\rm cr})$. Hence, the angle between the asymptote of this solution and the plane wave smoothly matching it can be only within this restricted interval. If the difference in properties of EM on the two sides of the semipenetrable boundary is so large that it would require an angle outside this interval, refraction is impossible. The wave front will break at the boundary, which may generate pairs of counter-rotating spiral waves. Similar considerations hold for the total internal reflection of autowaves described in [8].

In Sec. III we have shown that the existence of critical curvature destroys nonphysical self-crossings and loops of the solutions produced by the eikonal approximation. But the loops are replaced by singular cusps, which are also not physically realistic. By taking into account the unstable branch of the velocity-curvature relation, we believe it will be possible to remove the singular cusps. The pieces of the front constructing cusps may turn out to be smoothly connected with solutions supplied by the unstable branch. These fronts, though smooth and physically interpretable, would be unstable.

The unstable branch produced by Zykov's dependence (15) predicts zero velocity for the unstable plane front, but it is known [28,30] that the unstable pulse propagates with nonzero velocity. Numerical evaluations of $V(k)$ also indicate that the unstable branch crosses the V axis at some positive value [13,22,25]. A more realistic behavior of the unstable branch is shown in Fig. 2 by the dotted line. In Fig. 9 the orbit corresponding to the oscillating solution (27) is depicted together with its counterpart produced by the unstable branch. The trajectory flow is singular (nonunique) at the critical point. Here the stable wings of the solution, instead of being patched to each other, can be patched smoothly to the solution generated by the unstable branch, going through a region with high negative curvature (large loop in the half plane $k<0$). The resulting intrinsic equation $k(l)$ and corresponding front line are depicted qualitatively in Fig. 7 (solid and dotted lines together) and Fig. 10, respectively. The resulting front has to be unstable. We suspect that it has a close affinity with ''cellular'' flame fronts arising from an instability based on the interplay between thermal and molecular diffusivities [31], and with the development of unstable space-oscillating fronts in isothermal reaction-diffusion systems when the diffusivities of reactant and autocatalyst differ appropriately [32]. The study of time-dependent kinematics, which is currently underway, may shed light on the mechanism of formation and evolution of cusplike singularities.

V. CONCLUSIONS

We have found all noncirculating steady-state autowave front configurations in unbounded EM predicted by the kinematic model beyond the eikonal approximation. The nonlin-

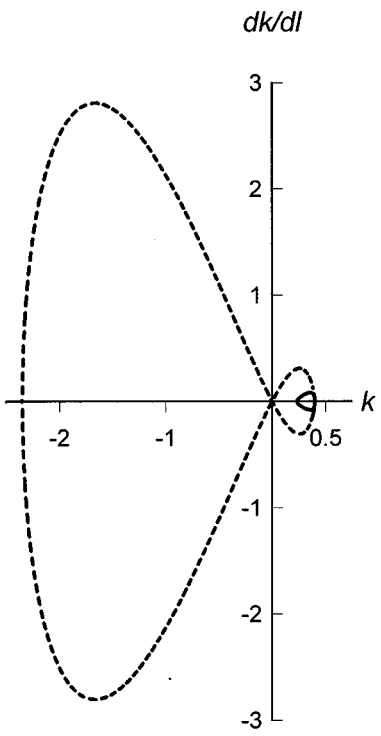

FIG. 9. The orbit of oscillating solution for stable branch of Zykov's dependence $V(k)$ is depicted by solid line $[V(0)=0.5]$. Dashed line denotes the portion of the orbit generated by the unstable branch in $V(k)$ shown in Fig. 2 by the dotted line. Other parameters as in Fig. 3.

ear dependence of local propagation velocity on curvature that we use contains a critical curvature beyond which the propagation of a continuous front is impossible. The better velocity-curvature relation does not change the number of

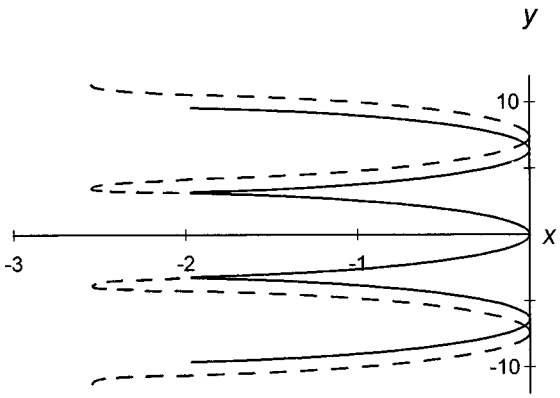

FIG. 10. The front lines corresponding to the oscillating solution (27) (dashed line) and to the oscillating solution accounting for the unstable branch in $V(k)$ (solid line).

propagating solutions found earlier in the eikonal approximation but does replace self-crossing solutions by solutions with singular cusps. We suggest that the unstable branch of the velocity-curvature relation may convert singular cusps into physically interpretable smooth cusps, but the front then becomes unstable.

We have shown that the effect of critical curvature puts restrictions on the range of allowable angles of reflected and refracted autowaves. Conditions which force the system to generate reflected-refracted angles beyond this region would cause the initially continuous front to break and reform as spiral waves.

ACKNOWLEDGMENTS

This work was supported by NSF Grant No. CHE 95-00763.

[1] *Wave and Patterns in Chemical and Biological Media*, edited by H. L. Swinney and V. I. Krinsky, special issue of Physica D 49 (1&2) (1991).
[2] M. C. Cross and P. C. Hohenberg, Rev. Mod. Phys. **65**, 851 (1993).
[3] *Chemical Waves and Patterns*, edited by R. Kapral and K. Showalter (Kluwer, Dordrecht, 1995).
[4] A. S. Mikhailov, *Foundations of Synergetics. I. Distributed Active Systems* (Springer-Verlag, Berlin, 1990).
[5] P. K. Brazhnik, Physica D **94**, 143 (1996).
[6] V. Pérez-Muñuzuri, M. Gómez-Gesteira, A. P. Muñuzuri, V. A. Davydov, and V. Pérez-Villar, Phys. Rev. E **51**, R845 (1995).
[7] P. K. Brazhnik and J. J. Tyson, Physica D (to be published); O. Steinbock, V. S. Zykov, and S. C. Muller, Phys. Rev. E **48**, 3295 (1993).
[8] P. K. Brazhnik and J. J. Tyson, Phys. Rev. E **54**, 1958 (1996).
[9] P. K. Brazhnik, V. A. Davydov, and A. S. Mikhailov, Teor. Mat. Fiz. **74**, 440 (1988) [Theor. Math. Phys. **74**, 300 (1988)].
[10] R. C. Brower, D. A. Kessler, J. Koplik, and H. Levin, Phys. Rev. A **29**, 1335 (1984); E. Ben-Jacob, N. Goldenfeld, J. S. Langer, and G. Schön, Physica D **12**, 245 (1984); P. Grindrod and J. Gomatam, J. Math. Biol. **25**, 597 (1987); P. Grindrod, M. A. Lewis, and J. D. Murray, Proc. R. Soc. London Ser. A **443**, 151 (1991); J. S. Wettlaufer, M. Jackson, and M. Elbaum, J. Phys. A **27**, 5957 (1994).
[11] J. P. Keener, SIAM **46**, 1039 (1986).
[12] J. P. Keener and J. J. Tyson, SIAM Rev. **34**, 1 (1992); M. E. Gurtin, *Thermodynamics of Evolving Phase Boundaries in the Plane* (Clarendon, Oxford, 1993).
[13] V. S. Zykov, *Simulation of Wave Processes in Excitable Media*, edited by A. T. Winfree (Manchester University Press, Manchester, 1987).
[14] A. S. Mikhailov and V. S. Zykov, Physica D **52**, 379 (1992).
[15] P. K. Brazhnik, V. A. Davydov, V. Pérez-Muñuzury, M. Gómez-Gesteira, A. P. Muñuzuri, C. Souto, and V. Pérez-Villar (unpublished).
[16] E. Meron and P. Pelce, Phys. Rev. Lett. **60**, 1880 (1988).
[17] P. K. Brazhnik and V. A. Davydov, Phys. Lett. A **199**, 40 (1995).
[18] V. A. Davydov, V. S. Zykov, A. S. Mikhailov, and P. K. Brazhnik, Izv. Vyssh. Uchebn. Zaved. Radiofiz. **31**, 574 (1988) [Radiophys. Quantum. Electron. **31**, 419 (1988)]; K. I. Agladze, V. A. Davydov, and A. S. Mikhailov, Pis'ma Zh.

Eksp. Teor. Fiz. **45**, 601 (1987) [JETP Lett. **45**, 767 (1987)].
[19] V. A. Davydov, V. S. Zykov, and A. S. Mikhailov, Physica D **70**, 1 (1994); E. Meron, Phys. Rep. **218**, 1 (1992).
[20] Since the EM recovers its properties after being excited, autowave fronts, as described by the kinematic theory, may have free ends inside the media.
[21] P. Foerster, S. Muller, and B. Hess, Science **241**, 685 (1988); Proc. Natl. Acad. Sci. U.S.A. **86**, 6831 (1989); Development **109**, 11 (1990); Z. Nagy-Ungvarai, J. Ungvarai, S. C. Muller and B. Hess, J. Chem. Phys. **97**, 1004 (1992).
[22] V. S. Zykov and O. L. Morozova, Biofizika **24**, 717 (1979) [Biophysics **24**, 739 (1979)].
[23] V. S. Zykov, Biofizika **25**, 896 (1980) [Biophysics **25**, 906 (1980)].
[24] J. P. Keener and J. J. Tyson, Physica D **21**, 307 (1986).
[25] J. Sneyd and A. Atri, Physica D **65**, 365 (1993); H. Ito, *ibid*. **79**, 16 (1994); M. Courtemanche, Chaos, Solitons Fractals **5**, 527 (1995).
[26] A. S. Mikhailov, Phys. Rev. E **49**, 5875 (1994); P. K. Brazhnik (unpublished).
[27] T. Yamaguchi, L. Kunhert, Zs. Nagy-Ungvaray, S. C. Müller, and B. Hess, J. Phys. Chem. **95**, 5831 (1991); M. Gómez-Gesteira, J. L. del Castillo, M. E. Vázquez-Iglesias, V. Pérez-Muñuzuri, and V. Pérez-Villar, Phys. Rev. E **50**, 4646 (1994).
[28] A. C. Scott, Rev. Mod. Phys. **47**, 47 (1975).
[29] Zykov's dependence $V(k)$ [Eq. (15)] also produces a branch in the fourth quadrant of the $\{V,k\}$ plane that does not have a physical meaning and therefore is not considered here.
[30] A. L. Hodgkin and A. F. Huxley, J. Physiol. **117**, 500 (1952); J. Rinzel and J. B. Keller, Biophys. J. **13**, 1313 (1973); R. N. Khramov and V. I. Krinskii, Biofizika **22**, 442 (1977) [Biophysics **22**, 512 (1977)].
[31] G. I. Sivashinsky, Combust. Sci. Technol. **15**, 137 (1977); M. L. Frankel and G. I. Sivashinsky, J. Phys. (Paris) **48**, 25 (1987).
[32] D. Horváth and K. Showalter, J. Chem. Phys. **102**, 2471 (1995); S. K. Scott and K. Showalter, in *Chemical Waves and Patterns* (Ref. [3]), p. 485; V. Petrov, Ph.D. thesis West Virginia University, Morgantown, 1995 (unpublished).